

Influence of cation on the cellulose dissolution investigated by MD simulation and experiments

Sen Wang · Kangjie Lyu · Peng Sun · Ang Lu · Maili Liu · Lin Zhuang · Lina Zhang

Received: 12 March 2017 / Accepted: 14 August 2017 / Published online: 18 August 2017
© Springer Science+Business Media B.V. 2017

Abstract Cellulose is the most abundant natural polymer on the earth, and effective solvents are essential for its wide application. Among various solvents such as alkali/urea or ionic liquids, cations all play a very important role on the cellulose dissolution. In this work, the influence of cation on the cellulose dissolution in alkali/urea via a cooling process was investigated with a combination of MD simulation and experiments, including differential scanning calorimetry (DSC) and NMR diffusometry (PFG-SE NMR). The results of DSC proved that the dissolution of cellulose in both solvents was a process within a temperature range, starting at above 0 °C and completing at low temperature (−5 °C for LiOH/urea and −20 °C for NaOH/urea), indicating the necessity of low temperature for the cellulose dissolution. Molecular dynamic (MD) simulation suggested that the electrostatic force between OH[−] and cellulose dominated the inter-molecular interactions. In our findings,

Li⁺ could penetrate closer to cellulose, and displayed stronger electrostatic interaction with the biomacromolecule than Na⁺, thus possessed a greater “stabilizing” effect on the OH[−]/cellulose interaction. PFG-SE NMR demonstrated a more significant binding fraction of Li⁺ than Na⁺ to cellulose, which was consistent with MD. These results indicated that the direct interactions existed between the cations and cellulose, and Li⁺ exhibited stronger interaction with cellulose, leading to stronger dissolving power.

Keywords Cellulose dissolution · Cation · Molecular dynamic simulation · PFG-SE NMR · Intermolecular interactions

Introduction

The world is currently consuming petroleum at a rate 100,000 times faster than nature can replace it (Netravali and Chabba 2003; Pinkert et al. 2009). Renewable resources, therefore, have attracted great attentions than ever before, due to the dilemma of depleting of fossil fuel and the pollution caused by petroleum-based materials. Cellulose, as the most abundant organic substance on earth, with renewability, low-cost, environmental friendliness, biocompatibility and biodegradability, is a promising candidate to produce environment-friendly materials (Klemm et al. 2005; Esaki et al. 2009; Wang et al. 2016). The

S. Wang · K. Lyu · A. Lu (✉) · L. Zhuang · L. Zhang (✉)
College of Chemistry and Molecular Sciences, Wuhan University, Wuhan 430072, China
e-mail: anglu@whu.edu.cn

L. Zhang
e-mail: zhangln@whu.edu.cn

P. Sun · M. Liu
State Key Laboratory of Magnetic Resonance and Atomic and Molecular Physics, Chinese Academy of Sciences, Wuhan 430071, China

processing progress, however, is difficult because of the existence of abundant intra- and inter-molecular hydrogen bonds, which lead to the cellulose hardly dissolved in common solvents or melt (Nishiyama et al. 2002). Finding effective solvents is essential for the wide application of cellulose. Several solvents have been developed to dissolve cellulose, such as lithium chloride/*N,N*-dimethylacetamide (Matsumoto et al. 2001; Chrapava et al. 2003) *N*-methylmorpholine-*N*-oxide, (Fink et al. 2001; Rosenau et al. 2001, 2002) ionic liquids etc. (Swatloski et al. 2002; Luo et al. 2012; Kosan et al. 2008). Recently, alkali/urea aqueous solvents have been developed, in which cellulose can be rapidly dissolved in 2 min with pre-cooling, revealing a completely new avenue to utilize the most intransigent biopolymer via a green technology (Zhang et al. 2002; Cai et al. 2008; Li et al. 2015b). The dissolving mechanism has attracted a lot of attention and been investigated from different aspects (Wang and Deng 2009; Bergensträhle-Wohler et al. 2012; Glasser et al. 2012; Xiong et al. 2014; Chen et al. 2017).

The cellulose dissolving capacity has been proved to differ among LiOH/urea, NaOH/urea and KOH/urea, namely LiOH/urea is stronger than NaOH/urea, but KOH/urea can hardly dissolve cellulose (Cai and Zhang 2005; Xiong et al. 2013). The phenomena suggest the great influences of the cations on the cellulose dissolution in the cooling solvents, as a result of the significant and unique interactions between the cations and the biopolymer. Several decades ago, CP/MAS ^{13}C was used at the temperature of 50–80 °C, to investigate the possible structure of alkalicellulose, in which the sodium ion was found to selectively coordinate to the hydroxyl oxygen at the C2 position of the glucose unit (Kamide et al. 1985). It should be noted that, the alkalicellulose sample was obtained by immersing cellulose in 18 wt% NaOH and aged at 49 °C for 30 h, which was quite different from the situation of dissolving cellulose with moderate NaOH solution at low temperature. Later, the structure of alkali solution was studied and some structure models were proposed. The study was well performed, mainly focused on the NaOH solution, and cellobiose as substitute of cellulose. The data of LiOH and cellulose was limited so that comparison was difficult to make (Yamashiki et al. 1988). In fact, the influences of cations on the dissolution of cellulose in other solvent systems are also prominent, and the mechanism has

been extensively studied in recent years (Yuan and Cheng 2015; Brendler et al. 2001; Payal and Balasubramanian 2014; Liu et al. 2016).

In the present work, the interactions between the ions and the cellulose macromolecules in the alkaline aqueous system were studied in various aspects such as differential scanning calorimetry (DSC), molecular dynamic (MD) simulation and nuclear magnetic resonance spectroscopy (NMR). We attempted to explain the reason why LiOH exhibits more powerful capacity in dissolving cellulose than NaOH, and why LiOH/urea was a preferred solvent for the dissolution of cellulose. The insights and comprehensive methods to investigate the ion-polymer interaction from the view of both experiments and simulation would also be provided for the help of future studies.

Experimental section

Materials

Cellulose (cotton linter pulps) with a certain degree of polymerization (DP = 465, 530 and 670, respectively, by viscometry (Brown and Wikström 1965)) and α -cellulose content of about 95% was supplied by Hubei Chemical Fiber Co. Ltd. (Xiangfan, China). The cellulose sample was vacuum-dried at 60 °C for 48 h to remove any moisture before use. Commercially available NaOH, LiOH·H₂O, KOH and urea were of analytical grade (Shanghai Chemical Reagent Co., China), and were used without further purification. The cellulose solvents were 7 wt% NaOH/12 wt% urea, 7.35 wt% LiOH·H₂O/12 wt% urea, 9.8 wt% KOH/12 wt% urea aqueous solution unless specifically indicated.

Characterization

Solubility test, a certain amount of cellulose was dispersed in NaOH/urea or LiOH/urea solvent pre-cooled to -12 °C and then stirred vigorously for 5 min. The mass of cellulose in the solution (m_s) and precipitate (m_p) were obtained after centrifugation at 8000 rpm at 0 °C for 15 min. The solubility (S) was then calculated according to (Zhou and Zhang 2000):

$$S = \frac{m_s}{m_s + m_p} \times 100\% \quad (1)$$

Differential scanning calorimetry (DSC) was conducted on a TA Q20 instrument. Cellulose was dispersed in the solvents and sealed in a stainless pan. The temperature was programmed from 35 °C to –60 °C and then –60 °C to 35 °C at a rate of 1 °C/min. The cycle was repeated for 3 times.

Nuclear magnetic resonance spectroscopy (NMR) spectra were recorded on a Bruker AVANCE III 500 NMR spectrometer with BBO probe at 273 K with external chemical-shift references. The concentration of cellulose solution was 3 wt%. The pulsed field-gradient spin-echo (PFG-SE) NMR method (Wu et al. 1995; Wang et al. 2017b) was used to quantitatively investigate the interaction of ions (Li^+ and Na^+) with macromolecule (cellulose) in the solution. Diffusion coefficients were extracted from nonlinear least squares of the integrated resonance intensity as a function of the gradient amplitude. The resonance intensity of these integrals, I , and the diffusion coefficient, D , are related according to the following equation:

$$I = I_0 \exp \left[-D \left(\Delta - \frac{\delta}{3} - \frac{\tau}{2} \right) g^2 \gamma^2 \delta^2 \right] \quad (2)$$

where I is the resonance intensity measure with pulse sequence, I_0 is the intensity of the resonance in the absence of a gradient pulse, D is the diffusion coefficient, Δ is the diffusion delay time, which defines the diffusional time scale, γ is the gyromagnetic ratio. The parameters δ and g are the gradient pulse duration and amplitude, respectively. And τ is the delay between the positive and negative gradient pulse. Because the γ for ^{23}Na and ^7Li is small, in order to get enough attenuation of signal intensity, Δ and δ equal to 30 ms, 14 ms for ^{23}Na NMR experiments and 70 ms, 7 ms for ^7Li NMR experiments, respectively.

TA Discovery Hybrid Rheometer (HR-2) was used for the rheology test. Temperature ramp was conducted under flow mode from 25 °C to –15 °C with ramp rate of 1 °C/min using 40 mm parallel plate. The parameter of velocity was 1.0 rad/s with sampling interval of 10.0 s/pt.

The atomistic molecular dynamic simulations were performed using the GROMACS software package (Hess et al. 2008). The GLYCAM06 force field was used to parameterize cellulose molecules (Kirschner et al. 2008). For water, the TIP3P model, (Jorgensen et al. 1983) and for OH^- , the model from Groenhof

were used, respectively (Wolf et al. 2014). For cations, the monovalent ion parameters (HFE set) for Particle Mesh Ewald and TIP3P water model from Merz were used (Li et al. 2015a). Parameters for cations modified by Lamoureux and Roux were also tried (Lamoureux and Roux 2006). The interaction of cations and OH^- was modified to reproduce a better rdf (radial distribution function) in their salt solution. The component is identical to the solvent system used in the experiments, which is 7 wt% NaOH/12 wt% urea or 7.35 wt% LiOH•H₂O/12 wt% urea. One periodically replicated cellulose octamer was considered, connected to its periodic images along the z-direction and thus mimicking an infinite chain, in the ion–water solution. The simulations were preceded by a 50 ns equilibration run and propagated for 30 ns with a time step of 2 fs. There were 100 ions and 3118 water in the box, with the size of (4.8 × 4.8 × 4.2). Long-range electrostatics were handled using the particle mesh Ewald method and the cut-off for short-range interactions was 1.0 nm. The temperature was kept at 273 K using the Berendsen thermostat and the pressure was kept at 1 bar using a weak coupling barostat independently applied in the xy- and z-directions (Berendsen et al. 1984).

Results and discussion

Dissolving capacity difference of solvents against cellulose

A quantitative comparison of the dissolution power against cellulose is summarized by measuring the solubility of cellulose with different molecular weights (M_w) in KOH/urea, NaOH/urea and LiOH/urea aqueous solutions, as shown in Table 1. LiOH/urea exhibited the strongest dissolving capacity, whereas cellulose hardly dissolve in KOH/urea. The solubility difference of cellulose is much larger at higher M_w , and LiOH/urea was capable of dissolving cellulose with higher M_w and/or higher concentration.

Dissolution of macromolecules was proved to be a process involved with thermal effect. The differential scanning calorimetry (DSC) was thus used to study the dissolution process of cellulose at low temperature with different cations. Figure 1 shows the DSC profile of cooling and heating cycles of cellulose mixed with NaOH/urea and LiOH/urea. During the cooling cycle,

Table 1 Solubility of cellulose with various molecular weights in LiOH/urea, NaOH/urea and KOH/urea


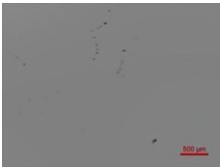
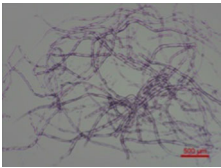
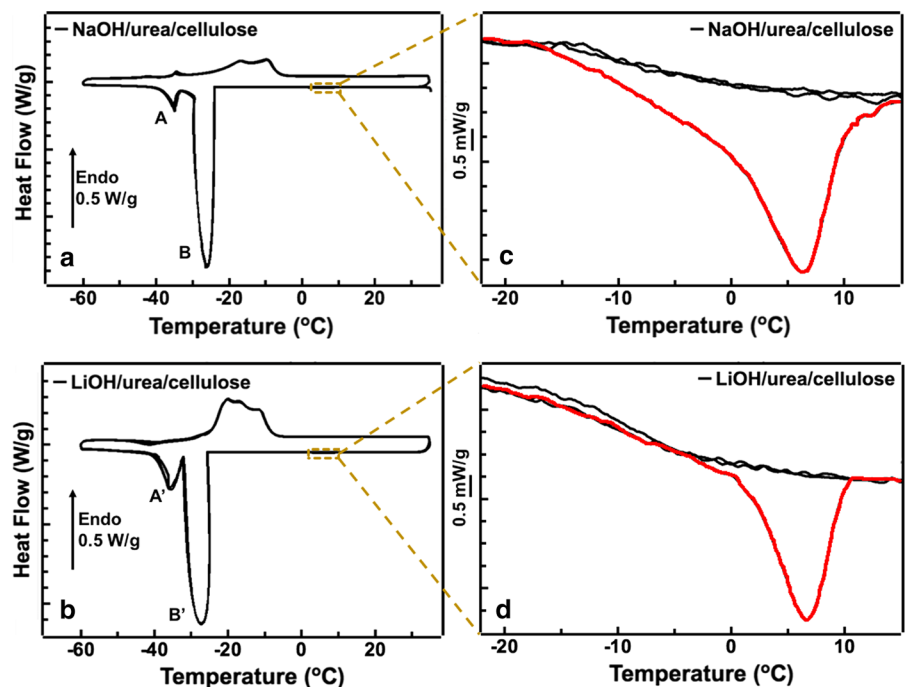
$M_w \times 10^{-4}$ (g/mol)	Solubility (wt%)		
			
11.0	84.1	70.0	—
8.6	92.9	83.6	—
7.6	95.1	93.1	—

Fig. 1 DSC profile of cooling and heating cycles of cellulose mixed with NaOH/urea (a, c) and LiOH/urea (b, d) solutions

two significant exothermic peaks (A, B and A', B') in each thermogram (at around -36 and -27 °C) were observed,

Ascribed to the freezing of NaOH or LiOH hydrate and urea hydrate which was overlapping, as well as freezing of bulk water, respectively. (Isobe et al. 2013) It was worth noting that the subtle exothermic peaks of the cellulose dissolution were revealed at around 0 °C. The exothermic peaks only appeared in the first cooling cycle for both NaOH/urea and LiOH/urea (highlighted by red lines), indicating that the complete

dissolution of cellulose could be achieved by merely cooling once. The cellulose dissolution peaks for both NaOH/urea and LiOH/urea started at >10 °C and reached the apexes at around 7 °C, however, ended with considerable differences. In LiOH/urea the cellulose dissolution completed at about -5 °C, whereas in NaOH/urea it completed at a much lower temperature at about -20 °C. Obviously, different cations resulted in the variance of the dissolving process. In order to further confirm the effects of the cations on cellulose dissolution, the rheological means

were conducted under the same cooling condition as DSC experiments for NaOH/urea and LiOH/urea, respectively.

Figure 2 shows the dependence of the steady shear viscosity of the mixture on the temperature change. During the cooling process, the gradual dissolution of cellulose causes an increase of the viscosity of the cellulose solution. The dissolution process monitored by rheology completed at a higher temperature than that by DSC, attributed to the shear applied during the rheological test, which promoted the disintegration of the cellulose chains. The viscosity for both cellulose/solvent mixtures encountered a sudden spurt at about 7 °C, indicating the dissolution of cellulose, which was consistent with the DSC profile. Therefore, the dissolution of cellulose at low temperature in both NaOH/urea and LiOH/urea was a typically enthalpy-driven process. It should be noted that the cellulose dissolution in both LiOH/urea and NaOH/urea was a process within a wide temperature range, which started at around 10 °C and completed at a temperature below 0 °C, in which low temperature is necessary. On the other hand, the cellulose dissolution in LiOH/urea and NaOH/urea completed at ~ -5 and -20 °C, respectively, attributed to the different interactions between cellulose and cations of Li^+ and Na^+ .

Interactions between alkali and cellulose by MD

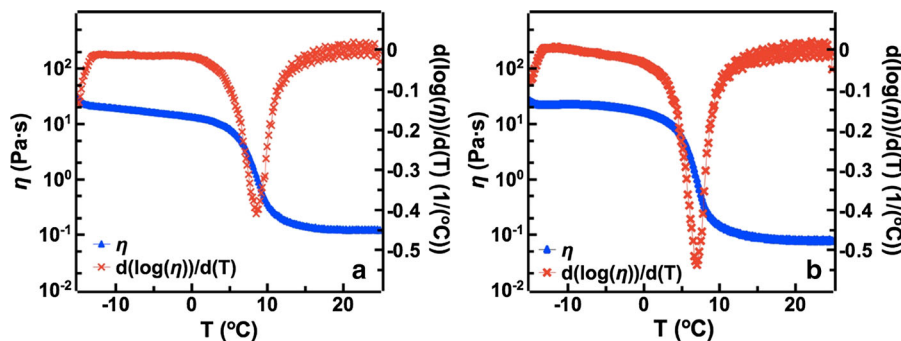
Solvent–solute interactions can be effectively revealed by molecular dynamic simulations (MD) to give useful information (Rabideau and Ismail 2015; Cai et al. 2012; Li et al. 2015c). Therefore, the atomistic molecular dynamic simulations were proposed here, focusing on the interactions between alkali and cellulose in the aqueous solution at low temperature. The potential energies between the components

in NaOH/cellulose and LiOH/cellulose was calculated and shown in Fig. 3. Among them, C–O, C–W and C–C represented the interactions between cellulose and OH^- , between cellulose and water, as well as between cellulose and cations, respectively. “Coul” and “LJ” denoted to electrostatic.

Interaction and van der Waals interaction, respectively. The potential energy of Li^+ /cellulose Coul interaction was 423 kJ/mol, larger than 212 kJ/mol of Na^+ /cellulose. The Coul OH^- /cellulose interaction in LiOH/cellulose was 2047 kJ/mol, also larger than 1324 kJ/mol of that in NaOH/cellulose, indicating a stronger interaction between OH^- /cellulose in LiOH than that in NaOH. It should be noted that the interaction in both LiOH/cellulose and NaOH/cellulose were mainly electrostatic, especially for the cellulose/ OH^- (C–O) and cations/cellulose (C–C). Therefore, the electrostatic interaction was dominant among the the interactions in the dissolved state. In addition, the Coul interaction potential energy of OH^- /cellulose was much larger than that of cations/cellulose, indicating Coul interaction of cellulose/ OH^- could be the dominating interaction in the cellulose dissolution among the several inter-molecular interactions. In fact, any sodium salts or lithium salts could not dissolve cellulose in the aqueous solution at low temperature without the OH^- . Therefore, the contribution from OH^- also played a role for the dissolution behavior. (Bialik et al. 2016).

Figure 4 shows the radial distribution function (RDF) of Li^+ , Na^+ and K^+ in the alkaline system to the O atoms of cellulose and their coordination number. The distance between the cations and the cellulose chains, however, showed difference for LiOH, NaOH and KOH. Li^+ ions laid at about 0.20 nm apart, while Na^+ ions laid at about 0.24 nm and K^+ ions laid at about 0.28. It should be noted that, the aqueous ionic radii of Li^+ (0.068 nm) was the

Fig. 2 Dependent of steady shear viscosity on temperature of cellulose/NaOH/urea **a** and cellulose/LiOH/urea **b** solutions with cooling



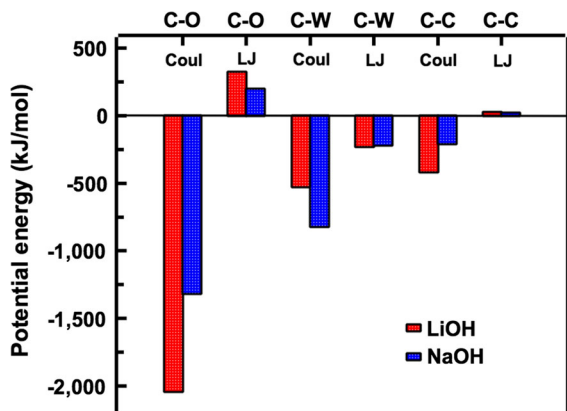


Fig. 3 Potential energy between cellulose and other components in LiOH (red) and NaOH (blue) solution, respectively. (Coul: electrostatic interaction, LJ: vdW interaction, C-O: cellulose–OH⁻, C-W: cellulose-water, C-C: cellulose-cation). (Color figure online)

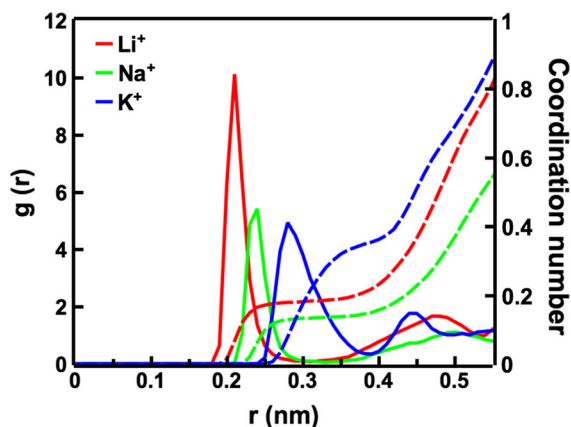


Fig. 4 Radial distribution function (RDF) of Li⁺, Na⁺ and K⁺ in the alkaline system to the O atoms of cellulose and their coordination number

smallest while K⁺ (0.134 nm) was the largest, (Marcus 1983) which may be related to their possibility to penetrate into the cellulose macromolecules. The RDF results indicated that, the interaction between cations and cellulose was different from Li⁺, Na⁺ and K⁺, in which, the Li⁺ ions had the strongest binding capacity with cellulose.

Figure 5 shows the RDF of cations to the oxygen atoms (O atoms) of cellulose in NaOH and LiOH. Cations including Na⁺ and Li⁺ interacted mostly intensively with the O6 and O3 of cellulose. In accordance with Fig. 4, all Na⁺ laid in the distance of 0.24 nm to cellulose, whereas a large part of Li⁺, due to a smaller radius, moved closer to the surface of the

cellulose chain, in the range of 0.20 nm to the O atoms of cellulose. The result was in accordance with the data in Fig. 3, in which a stronger electrostatic interaction between Li⁺ and cellulose was demonstrated, leading to a larger positive potential energy of Li⁺/cellulose LJ interaction, which implied a smaller distance between Li⁺ and cellulose chains. This was quite crucial to a stronger dissolving ability of LiOH than NaOH against cellulose. The OH⁻/cellulose Coul interaction, as up-mentioned, dominated the intermolecular interactions between alkali and cellulose, however, such interaction was not fully stable. Figure 6 displays the snapshot captured during the simulation as an example, illustrating the “stabilization” of OH⁻ to cellulose.

Chain by the nearby Li⁺. The OH⁻ interacted mostly with the hydroxyls of the cellulose, and most of them maintained a stable interaction with the cellulose chain except for the highlighted ones. Among the highlighted Li⁺ (blue) and two OH⁻ (red/white), Li⁺ “stabilized” the adjacent OH⁻, maintaining its interaction with the cellulose in the next frame, while the OH⁻ without the stabilization of Li⁺ detached from the surface of the cellulose chain. Na⁺, however, are relatively farther from the cellulose chain than Li⁺, and their interaction with the cellulose was weaker. Thus their stabilizing ability.

Towards OH⁻ to maintain the breaking up of hydrogen bonding of cellulose was less effective, leading to the more powerful dissolving capacity of LiOH than NaOH. To conclude in this part, the MD results revealed that OH⁻/cellulose electrostatic interaction dominated among the dissolved state by forming the strongest interaction with the hydroxyl groups of the cellulose chain among the intermolecular interactions, and cations also electrostatically interacted with the cellulose O atoms. Li⁺ attached with the cellulose closely and interacted stronger with cellulose chains than Na⁺, and exhibited a greater “stabilizing” effect on the electrostatic OH⁻/cellulose interaction in LiOH/cellulose than NaOH/cellulose, thus leading to the more powerful dissolving capacity of LiOH than NaOH against cellulose.

Binding of cations to cellulose in alkali/urea by PFG-SE NMR

As mentioned above, the cations of alkalis, *i.e.*, Na⁺ and Li⁺ were proved to interact directly with the

Fig. 5 RDF of cations to the O atoms of cellulose in NaOH (a) and LiOH (b)

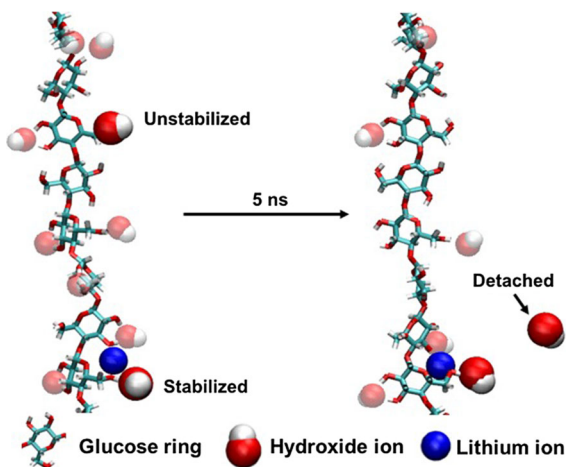
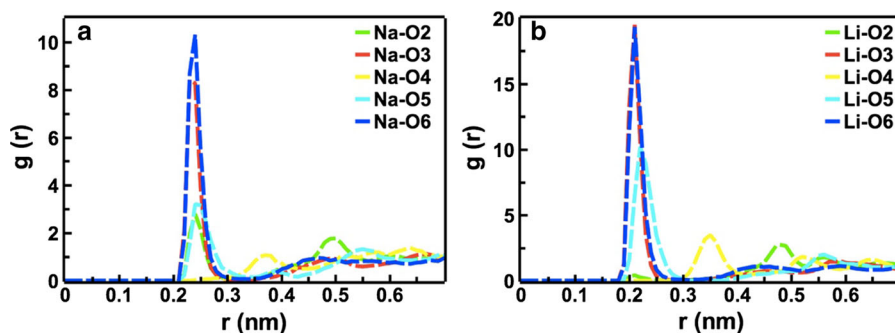
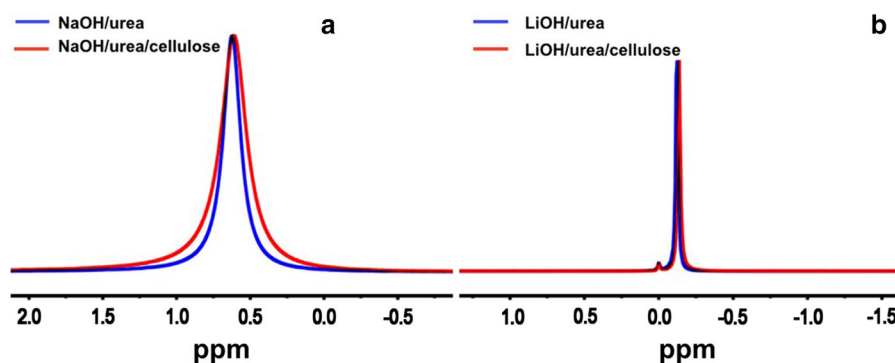


Fig. 6 A snapshot to illustrate the “stabilization” of hydroxide ions to attach to cellulose chain by the nearby Li^+ ion

cellulose chains at low temperature from the view of molecular simulation. In the following part, NMR as an effective method (Zhang et al. 2010; Wang et al. 2017a) was then used to further validate the influences of cations on the cellulose from the experimental view.

Figure 7 shows the ^{23}Na spectroscopy of NaOH/urea solvent and NaOH/urea/cellulose solution, as

Fig. 7 ^{23}Na NMR spectra of NaOH/urea, NaOH/urea/cellulose solution (a) and ^7Li spectra of LiOH/urea, LiOH/urea/cellulose solution (b)

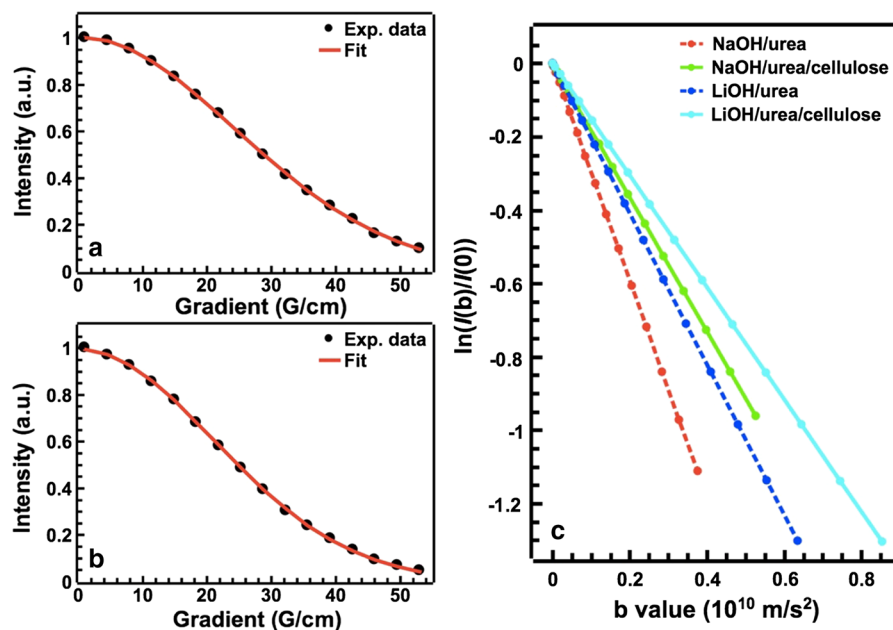


well as the ^7Li spectroscopy of LiOH/urea solvent and LiOH/urea/cellulose solution. The peaks of both Na^+ and Li^+ exhibited similarity with the addition of cellulose, by moving slightly to a higher field. However, the shifts could hardly be quantitatively compared since the involvement of two different nuclei and the chemical shifts are usually fairly small due to their “not easily polarized” characters (Templeman and Van Geet 1972). Thus, pulsed field-gradient spin-echo (PFG-SE) NMR were applied to obtain the self-diffusion coefficients of the ions, in order to clarify the interactions between different cations and cellulose in alkali/urea systems, as shown in Fig. 8. For the cellulose/cation binding equilibria in fast exchange on the NMR diffusion time scale, the observed self-diffusion coefficients (D_o) is a weighted average which can be expressed by the following equation:

$$D_o = F_f D_f + F_b D_b \quad (3)$$

where F_f is the fraction of the free cation, F_b is the fraction of the bound cation, D_f is the diffusion coefficient of the free cation, D_b is the diffusion coefficient of the bound cation, which was nearly equal to be the diffusion coefficient of cellulose (D_c)

Fig. 8 Fit lines of the normalized intensity versus gradient in the NMR diffusometry of NaOH/urea/cellulose (a) and LiOH/urea/cellulose (b). (c) Typical ^{23}Na and ^7Li NMR signal decay as function of diffusion attenuation factor in NaOH/urea and LiOH/urea solutions in absence and presence of 3 wt% cellulose ($b = (\gamma g \delta)^2 (\Delta - \delta/3)$)



due to their combination. The chemical shift reflected the average status of the overall cations in the solution, therefore, the little variation shown in Fig. 7 implied a small fraction of binding ions (F_b). Also, the diffusion coefficient of the free ions was much larger than that of the macromolecular cellulose (D_c) ($D_b \approx D_c \ll D_f$). So the Eq. (1) can be simplified as:

$$D_o = F_f D_f \quad (4)$$

According to the Stokes–Einstein equation, viscosity is inversely proportional to the diffusion coefficient. Since water took up most part in the solution, its diffusion should be considered as only related to the viscosity of the solution, and the effect of interaction between water and cellulose on its D value was negligible. The determination of changes in the diffusion coefficient of the cations due to the viscosity changes of the solution resulting from the addition of cellulose was therefore corrected by the diffusion coefficient of water molecules, summarized in Table 2.

Based on the facts that only one peak was observed for both ^7Li NMR and ^{23}Na NMR (Fig. 7), and their intensities followed a single exponential decay in the PFG-SE experiment (Fig. 8a, b), we could reasonably assume that the binding of Li^+ and Na^+ with cellulose was fast in NMR time scale and the fraction of bound form could be derived from the viscosity corrected

Table 2 Diffusion coefficients of H_2O and cations by PFG-SE NMR

	$D \times 10^{10} \text{ (m}^2/\text{s)}$		
	H_2O	Na^+	Li^+
NaOH/urea	6.837	3.807	–
NaOH/urea/cellulose	6.032	3.197	–
LiOH/urea	5.265	–	2.111
LiOH/urea/cellulose	4.434	–	1.525

D value. Figure 8c shows the typical ^{23}Na and ^7Li NMR signal decay as function of diffusion attenuation factor in NaOH/urea and LiOH/urea solutions in absence and presence of 3 wt% cellulose. The slope of the fitted lines indicated the $(-D)$ value. Even without cellulose, obviously, Li^+ in LiOH/urea exhibited a smaller diffusion coefficient than Na^+ in NaOH/urea,

Suggesting the larger hydrated radius of the lithium ions (Kielland 1937). The addition of cellulose resulted in that both the diffusion coefficients of Na^+ and Li^+ reduced, indicating the binding of cations with the cellulose. This could be explained by the electrostatic interactions between cations and cellulose revealed by MD in the former section. The F_b of Na^+ was then calculated to be 4.8% while F_b of Li^+ was 14.2%, nearly twice more. The results thus gave

direct and definitively quantitative data, demonstrating that Li^+ had a much more significant binding capability to the macromolecular chains of cellulose than Na^+ . Therefore, the direct interactions between cations and cellulose did exist, however, due to the low portion of the interacted cations it was not obviously detected by chemical shift of NMR test. On the contrary, PFG-SE NMR was capable of detecting the interactions between them and supply quantitative results. It was also indicated that the interaction between Li^+ and cellulose was stronger than that of Na^+ , validating the conclusion of MD simulation. Generally speaking, the interaction between the ion and polymer involves several possibilities, including direct interactions between the ion and a polar group on the polymer chain, or indirect interactions through the change in the water structure influencing the hydration shell of both the polymer and the ions. It has been concluded that the interaction between cations and cellulose were mainly electrostatic from the MD results with Li^+ /cellulose Coul interaction much stronger than Na^+ /cellulose, and the NMR diffusometry showed a more significant binding fraction of Li^+ than Na^+ . Thus it could be deduced that the direct interactions between the cations and cellulose existed and Li^+ exhibited stronger interaction with cellulose than Na^+ , in consistence with the MD results, which played a very important role in the cellulose dissolution at low temperature in alkali/urea solvents. The stronger binding of Li^+ to cellulose could also “stabilize” OH^- /cellulose Coul interaction and promote to break up the hydrogen bonding between the cellulose chains by OH^- , leading to a more significant dissolving capacity of LiOH/urea than NaOH/urea.

Conclusion

The cellulose dissolution in LiOH/urea and NaOH/urea were completed with different behavior, implying the influence of different cations of Li^+ and Na^+ . The MD simulation suggested that electrostatic interaction of OH^- ions with cellulose dominated among the interactions in the dissolved state, and the cations also electrostatically interacted with cellulose. Moreover, Li^+ penetrated closer to cellulose than Na^+ , leading to a more significant “stabilizing” role of the electrostatic interaction between OH^- of the alkali and cellulose.

Experimentally, the stronger binding ability of Li^+ to cellulose evidenced by NMR diffusometry was consistent with the MD results, suggesting that the direct interactions existed between the cations and cellulose.

Acknowledgment This work was supported by the Major Program of National Natural Science Foundation of China (21334005), the Major International (Regional) Joint Research Project (21620102004) and the National Natural Science Foundation of China (51573143, 51203122 and 21505153).

References

- Berendsen HJC, Postma JPM, van Gunsteren WF et al (1984) Molecular dynamics with coupling to an external bath. *J Chem Phys* 81:3684–3690. doi:10.1063/1.448118
- Bergensträhle-Wohlert M, Berglund LA, Brady JW et al (2012) Concentration enrichment of urea at cellulose surfaces: results from molecular dynamics simulations and NMR spectroscopy. *Cellulose* 19:1–12. doi:10.1007/s10570-011-9616-x
- Bialik E, Stenqvist B, Fang Y et al (2016) Ionization of cellobiose in aqueous alkali and the mechanism of cellulose dissolution. *J Phys Chem Lett* 7:5044–5048. doi:10.1021/acs.jpcclett.6b02346
- Brendler E, Fischer S, Leipner H (2001) ^7Li NMR as probe for solvent–cellulose interactions in cellulose dissolution. *Cellulose* 8:283–288. doi:10.1023/A:1015120107514
- Brown W, Wikström R (1965) A viscosity-molecular weight relationship for cellulose in cadoxen and a hydrodynamic interpretation. *Eur Polym J* 1:1–10. doi:10.1016/0014-3057(65)90041-8
- Cai J, Zhang L (2005) Rapid dissolution of cellulose in LiOH/Urea and NaOH/Urea aqueous solutions. *Macromol Biosci* 5:539–548. doi:10.1002/mabi.200400222
- Cai J, Zhang L, Liu S et al (2008) Dynamic self-assembly induced rapid dissolution of cellulose at low temperatures. *Macromolecules* 41:9345–9351
- Cai L, Liu Y, Liang H (2012) Impact of hydrogen bonding on inclusion layer of urea to cellulose: study of molecular dynamics simulation. *Polymer* 53:1124–1130. doi:10.1016/j.polymer.2012.01.008
- Chen P, Nishiyama Y, Wohlert J et al (2017) Translational entropy and dispersion energy jointly drive the adsorption of urea to cellulose. *J Phys Chem B* 121:2244–2251. doi:10.1021/acs.jpcc.6b11914
- Chrapava S, Touraud D, Rosenau T et al (2003) The investigation of the influence of water and temperature on the LiCl/DMAc/cellulose system. *Phys Chem Chem Phys* 5:1842–1847. doi:10.1039/B212665F
- Esaki K, Yokota S, Egusa S et al (2009) Preparation of lactose-modified cellulose films by a nonaqueous enzymatic reaction and their biofunctional characteristics as a scaffold for cell culture. *Biomacromol* 10:1265–1269
- Fink HP, Weigel P, Purz HJ, Ganster J (2001) Structure formation of regenerated cellulose materials from NMMO-solutions. *Prog Polym Sci* 26:1473–1524

- Glasser WG, Atalla RH, Blackwell J et al (2012) About the structure of cellulose: debating the Lindman hypothesis. *Cellulose* 19:589–598. doi:[10.1007/s10570-012-9691-7](https://doi.org/10.1007/s10570-012-9691-7)
- Hess B, Kutzner C, van der Spoel D, Lindahl E (2008) GRO-MACS 4: algorithms for highly efficient, load-balanced, and scalable molecular simulation. *J Chem Theory Comput* 4:435–447. doi:[10.1021/ct700301q](https://doi.org/10.1021/ct700301q)
- Isobe N, Noguchi K, Nishiyama Y et al (2013) Role of urea in alkaline dissolution of cellulose. *Cellulose* 20:97–103. doi:[10.1007/s10570-012-9800-7](https://doi.org/10.1007/s10570-012-9800-7)
- Jorgensen WL, Chandrasekhar J, Madura JD et al (1983) Comparison of simple potential functions for simulating liquid water. *J Chem Phys* 79:926–935. doi:[10.1063/1.445869](https://doi.org/10.1063/1.445869)
- Kamide K, Kowsaka K, Okajima K (1985) Determination of intramolecular hydrogen bonds and selective coordination of sodium cation in alkal cellulose by CP/MASS 13C NMR. *Polym J* 17:707–711
- Kielland J (1937) Individual activity coefficients of ions in aqueous solutions. *J Am Chem Soc* 59:1675–1678. doi:[10.1021/ja01288a032](https://doi.org/10.1021/ja01288a032)
- Kirschner KN, Yongye AB, Tschampel SM et al (2008) GLY-CAM06: a generalizable biomolecular force field. *Carbohydrates. J Comput Chem* 29:622–655. doi:[10.1002/jcc.20820](https://doi.org/10.1002/jcc.20820)
- Klemm D, Heublein B, Fink H-P, Bohn A (2005) Cellulose: fascinating biopolymer and sustainable raw material. *Angew Chem Int Ed* 44:3358–3393
- Kosan B, Michels C, Meister F (2008) Dissolution and forming of cellulose with ionic liquids. *Cellulose* 15:59–66
- Lamoureux G, Roux B (2006) Absolute hydration free energy scale for alkali and halide ions established from simulations with a polarizable force field. *J Phys Chem B* 110:3308–3322. doi:[10.1021/jp056043p](https://doi.org/10.1021/jp056043p)
- Li P, Song LF, Merz KM (2015a) Systematic parameterization of monovalent ions employing the nonbonded model. *J Chem Theory Comput* 11:1645–1657. doi:[10.1021/ct500918t](https://doi.org/10.1021/ct500918t)
- Li R, Wang S, Lu A, Zhang L (2015b) Dissolution of cellulose from different sources in an NaOH/urea aqueous system at low temperature. *Cellulose* 22:339–349. doi:[10.1007/s10570-014-0542-6](https://doi.org/10.1007/s10570-014-0542-6)
- Li Y, Liu X, Zhang S et al (2015c) Dissolving process of a cellulose bunch in ionic liquids: a molecular dynamics study. *Phys Chem Chem Phys* 17:17894–17905. doi:[10.1039/C5CP02009C](https://doi.org/10.1039/C5CP02009C)
- Liu Z, Zhang C, Liu R et al (2016) Dissolution of cellobiose in the aqueous solutions of chloride salts: hofmeister series consideration. *Cellulose* 23:295–305. doi:[10.1007/s10570-015-0827-4](https://doi.org/10.1007/s10570-015-0827-4)
- Luo N, Lv Y, Wang D et al (2012) Direct visualization of solution morphology of cellulose in ionic liquids by conventional TEM at room temperature. *Chem Commun* 48:6283–6285. doi:[10.1039/C2CC31483E](https://doi.org/10.1039/C2CC31483E)
- Marcus Y (1983) Ionic radii in aqueous solutions. *J Solut Chem* 12:271–275. doi:[10.1007/BF00646201](https://doi.org/10.1007/BF00646201)
- Matsumoto T, Tatsumi D, Tamai N, Takaki T (2001) Solution properties of celluloses from different biological origins in LiCl-DMAc. *Cellulose* 8:275–282. doi:[10.1023/A:1015162027350](https://doi.org/10.1023/A:1015162027350)
- Netravali AN, Chabba S (2003) Composites get greener. *Mater Today* 6:22–29. doi:[10.1016/S1369-7021\(03\)00427-9](https://doi.org/10.1016/S1369-7021(03)00427-9)
- Nishiyama Y, Langan P, Chanzy H (2002) Crystal structure and hydrogen-bonding system in cellulose I β from synchrotron X-ray and neutron fiber diffraction. *J Am Chem Soc* 124:9074–9082. doi:[10.1021/ja0257319](https://doi.org/10.1021/ja0257319)
- Payal RS, Balasubramanian S (2014) Dissolution of cellulose in ionic liquids: an ab initio molecular dynamics simulation study. *Phys Chem Chem Phys* 16:17458–17465. doi:[10.1039/C4CP02219J](https://doi.org/10.1039/C4CP02219J)
- Pinkert A, Marsh KN, Pang S, Staiger MP (2009) Ionic liquids and their interaction with cellulose. *Chem Rev* 109:6712–6728
- Rabideau BD, Ismail AE (2015) Mechanisms of hydrogen bond formation between ionic liquids and cellulose and the influence of water content. *Phys Chem Chem Phys* 17:5767–5775. doi:[10.1039/C4CP04060K](https://doi.org/10.1039/C4CP04060K)
- Rosenau T, Potthast A, Sixta H, Kosma P (2001) The chemistry of side reactions and byproduct formation in the system NMMO/cellulose (Lyocell process). *Prog Polym Sci* 26:1763–1837
- Rosenau T, Potthast A, Adorjan I et al (2002) Cellulose solutions in *N*-methylmorpholine-*N*-oxide (NMMO)–degradation processes and stabilizers. *Cellulose* 9:283–291
- Swatloski RP, Spear SK, Holbrey JD, Rogers Robin D (2002) Dissolution of cellulose with ionic liquids. *J Am Chem Soc* 124:4974–4975
- Templeman GJ, Van Geet AL (1972) Sodium magnetic resonance of aqueous salt solutions. *J Am Chem Soc* 94:5578–5582. doi:[10.1021/ja00771a008](https://doi.org/10.1021/ja00771a008)
- Wang Y, Deng Y (2009) The kinetics of cellulose dissolution in sodium hydroxide solution at low temperatures. *Biotechnol Bioeng* 102:1398–1405. doi:[10.1002/bit.22160](https://doi.org/10.1002/bit.22160)
- Wang S, Lu A, Zhang L (2016) Recent advances in regenerated cellulose materials. *Prog Polym Sci* 53:169–206. doi:[10.1016/j.progpolymsci.2015.07.003](https://doi.org/10.1016/j.progpolymsci.2015.07.003)
- Wang S, Sun P, Liu M et al (2017a) Weak interactions and their impact on cellulose dissolution in an alkali/urea aqueous system. *Phys Chem Chem Phys* 19:17909–17917. doi:[10.1039/C7CP02514A](https://doi.org/10.1039/C7CP02514A)
- Wang S, Sun P, Zhang R et al (2017b) Cation/macromolecule interaction in alkaline cellulose solution characterized with pulsed field-gradient spin-echo NMR spectroscopy. *Phys Chem Chem Phys* 19:7486–7490. doi:[10.1039/C6CP08744B](https://doi.org/10.1039/C6CP08744B)
- Wolf MG, Grubmüller H, Groenhof G (2014) Anomalous surface diffusion of protons on lipid membranes. *Biophys J* 107:76–87. doi:[10.1016/j.bpj.2014.04.062](https://doi.org/10.1016/j.bpj.2014.04.062)
- Wu DH, Chen AD, Johnson CS (1995) An improved diffusion-ordered spectroscopy experiment incorporating bipolar-gradient pulses. *J Magn Reson A* 115:260–264. doi:[10.1006/jmra.1995.1176](https://doi.org/10.1006/jmra.1995.1176)
- Xiong B, Zhao P, Cai P et al (2013) NMR spectroscopic studies on the mechanism of cellulose dissolution in alkali solutions. *Cellulose* 20:613–621
- Xiong B, Zhao P, Hu K et al (2014) Dissolution of cellulose in aqueous NaOH/urea solution: role of urea. *Cellulose* 21:1183–1192. doi:[10.1007/s10570-014-0221-7](https://doi.org/10.1007/s10570-014-0221-7)
- Yamashiki T, Kamide K, Okajima K et al (1988) Some characteristic features of dilute aqueous alkali solutions of specific alkali concentration (2.5 mol l⁻¹) which possess maximum solubility power against cellulose. *Polym J* 20:447–457

- Yuan X, Cheng G (2015) From cellulose fibrils to single chains: understanding cellulose dissolution in ionic liquids. *Phys Chem Chem Phys* 17:31592–31607. doi:[10.1039/C5CP05744B](https://doi.org/10.1039/C5CP05744B)
- Zhang L, Ruan D, Gao S (2002) Dissolution and regeneration of cellulose in NaOH/thiourea aqueous solution. *J Polym Sci, Part B: Polym Phys* 40:1521–1529. doi:[10.1002/polb.10215](https://doi.org/10.1002/polb.10215)
- Zhang J, Zhang H, Wu J et al (2010) NMR spectroscopic studies of cellobiose solvation in EmimAc aimed to understand the dissolution mechanism of cellulose in ionic liquids. *Phys Chem Chem Phys* 12:1941–1947. doi:[10.1039/B920446F](https://doi.org/10.1039/B920446F)
- Zhou J, Zhang L (2000) Solubility of cellulose in NaOH/Urea aqueous solution. *Polym J* 32:866–870. doi:[10.1295/polymj.32.866](https://doi.org/10.1295/polymj.32.866)